

 Open access • Journal Article • DOI:10.1063/1.2713861

## Liquid-crystal-based linear polarization rotator — Source link

Hongwen Ren, Shin-Tson Wu

**Published on:** 21 Mar 2007 - Applied Physics Letters (American Institute of Physics)

**Topics:** Polarization rotator, Optic axis of a crystal, Elliptical polarization, Waveplate and Linear polarization

Related papers:

- [Liquid crystal device for control of polarized light](#)
- [Polarized light separating element and its production](#)
- [Anti-ferroelectric liquid crystal display with twisted director and perpendicular smectic layers](#)
- [Light reflection film](#)
- [Optical system, liquid crystal element, and method for manufacturing liquid crystal element](#)

Share this paper:    

View more about this paper here: <https://typeset.io/papers/liquid-crystal-based-linear-polarization-rotator-3ru8wln8sx>

1-1-2007

## Liquid-crystal-based linear polarization rotator

Hongwen Ren  
*University of Central Florida*

Shin-Tson Wu  
*University of Central Florida*

Find similar works at: <https://stars.library.ucf.edu/facultybib2000>  
University of Central Florida Libraries <http://library.ucf.edu>

This Article is brought to you for free and open access by the Faculty Bibliography at STARS. It has been accepted for inclusion in Faculty Bibliography 2000s by an authorized administrator of STARS. For more information, please contact [STARS@ucf.edu](mailto:STARS@ucf.edu).

---

### Recommended Citation

Ren, Hongwen and Wu, Shin-Tson, "Liquid-crystal-based linear polarization rotator" (2007). *Faculty Bibliography 2000s*. 7565.  
<https://stars.library.ucf.edu/facultybib2000/7565>

# Liquid-crystal-based linear polarization rotator

Cite as: Appl. Phys. Lett. **90**, 121123 (2007); <https://doi.org/10.1063/1.2713861>

Submitted: 09 January 2007 . Accepted: 10 February 2007 . Published Online: 21 March 2007

Hongwen Ren, and Shin-Tson Wu



View Online



Export Citation

## ARTICLES YOU MAY BE INTERESTED IN

[Achromatic linear polarization rotator using twisted nematic liquid crystals](#)

Applied Physics Letters **76**, 3995 (2000); <https://doi.org/10.1063/1.126846>

[A perfect metamaterial polarization rotator](#)

Applied Physics Letters **103**, 171107 (2013); <https://doi.org/10.1063/1.4826536>

[90° polarization rotator using a bilayered chiral metamaterial with giant optical activity](#)

Applied Physics Letters **96**, 203501 (2010); <https://doi.org/10.1063/1.3429683>

**MMR TECHNOLOGIES**

**THE WORLD'S RESOURCE FOR  
VARIABLE TEMPERATURE  
SOLID STATE CHARACTERIZATION**

[WWW.MMR-TECH.COM](http://WWW.MMR-TECH.COM)

OPTICAL STUDIES SYSTEMS    SQUID STUDIES SYSTEMS    MICROPROB STATIONS    HALL EFFECT STUDY SYSTEMS AND MAGNETS

## Liquid-crystal-based linear polarization rotator

Hongwen Ren and Shin-Tson Wu<sup>a)</sup>

*College of Optics and Photonics, University of Central Florida, Orlando, Florida 32816*

(Received 9 January 2007; accepted 10 February 2007; published online 21 March 2007)

A liquid-crystal (LC)-based polarization rotator which can rotate the polarization axis of an incident linearly polarized light from  $0^\circ$  to  $90^\circ$  is demonstrated. In the LC cell, the top substrate has a uniform rubbing but the bottom substrate has two orthogonal rubbings which are separated by a nonrubbing zone. Between these two rubbed strips, the LC directors twist continuously from  $0^\circ$  to  $90^\circ$ . As a result, the optic axis of the incident linearly polarized light can be rotated continuously depending on the beam position. © 2007 American Institute of Physics. [DOI: 10.1063/1.2713861]

A liquid-crystal (LC)-based polarization converter is an intriguing optical device because it can convert a linearly polarized light into circular, elliptical, axial, radial, or azimuthal polarization depending on the LC configurations.<sup>1-7</sup> If the employed LC presents a homogeneous alignment,<sup>1</sup> then it can generate linear, circular, or elliptical polarization by controlling the applied voltage. On the other hand, if the LC has radial or twisted radial orientation, then a space-variant output light with axial, radial, or azimuthal polarization can be generated. However, there is still lack of LC converter that can continuously rotate the optic axis of a linearly polarized light. Such a LC polarization converter would be used as a polarization axis finder, phase modulator for analyzing biological tissues and polarizing materials, diffractive optics, and other optical elements.

Nematic LC molecules have rodlike structures and their directors can be reoriented either by electric field, rubbing treatment, or both. If the LC directors are twisted,<sup>8</sup> then the device can rotate the optic axis of a linearly polarized light due to the waveguiding effect. Here, we call such a converter a polarization rotator. Various LC rotators based on different LC configurations have been proposed. For example, Yamaguchi *et al.*<sup>2</sup> demonstrated a LC polarization rotator by controlling the azimuthal anchoring strength of the LC cell with different UV exposures. After rubbing treatment, they demonstrated a LC rotator with multiple twist angle patterning. A LC rotator using such a fabrication method causes two concerns: discontinuous twist angle and complicated fabrication process. A linear polarization rotator which can continuously twist the plane of a linearly polarized light can be widely used in optical splitters, variable filters, optical data storage, grating, and other optical elements.

In this letter, we demonstrate a LC-based linear polarization rotator using a simple rubbing method. Our device can rotate the optic axis of an incident linearly polarized light spatially. The major advantages of our approach are twofold: simple fabrication process and large size capability. Moreover, using this method a polarization rotator array can be fabricated easily.

To achieve a continuous twist from  $0^\circ$  to  $90^\circ$ , we fabricated the LC cell as follows. The top glass substrate surface was coated with a thin polyimide (PI) layer and rubbed along the  $-x$  axis, as shown in Fig. 1. The bottom substrate surface was divided into the left, middle, and right regions; each

region had different rubbing treatments. In the first step, we rubbed the left part of the bottom substrate along the  $y$  axis while keeping the middle and right regions covered with a thin glass plate. We then rubbed the right strip along the  $x$  axis while keeping the middle and left strips covered. Afterwards, we assembled these two substrates together to form a cell. The cell consists of three different regions corresponding to the surface treatments of the bottom substrate. In the left region, the rubbing directions of the top and bottom substrates are perpendicular while in the right region the rubbing directions are antiparallel. In the middle region, only the top surface has rubbing.

When a LC material was filled to the cell, the LC molecules were aligned by the rubbed surfaces. Figure 2 depicts the schematic side view of the ideal LC configurations in the cell. From left to right, the cell is divided into three zones. Positions A and B represent the edges of the nonrubbed region. Induced by the two rubbed surfaces, the LC directors in the left region exhibit a  $90^\circ$  twist while in the right region they are homogeneous. Between A and B, the LC directors on the top surface are homogeneously aligned along the rubbing direction due to the strong anchoring force of the PI layer. But the LC directors near the bottom substrate surface would twist continuously from  $90^\circ$  to  $0^\circ$ , as depicted in Fig. 2. Because of the weak anchoring energy of the bottom glass surface which has no PI layer, the LC directors in the non-rubbing region are influenced by the LCs in the left and right regions. Moreover, the LC is a continuum medium. In an equilibrium state, the boundary layers in the bottom substrate gradually twist. As a result, the bulk LC directors between A and B gradually transition from  $90^\circ$  twist to homogeneous, as Fig. 2 depicts.

In Fig. 2 when a linearly polarized light is incident normally to the LC cell with its polarization direction parallel to the  $x$  axis, the transmitted light remains linearly polarized but its polarization axis follows the LC director twist, provided that the following Mauguin condition is satisfied:<sup>9</sup>

$$2\pi d\Delta n/\lambda \gg \phi. \quad (1)$$

In Eq. (1),  $\phi$  is the twist angle,  $d$  is the LC layer thickness,  $\Delta n$  is the LC birefringence, and  $\lambda$  is the wavelength. For a  $90^\circ$  twisted nematic cell,  $\phi = \pi/2$  and the Mauguin condition is simplified to

<sup>a)</sup>Electronic mail: swu@mail.ucf.edu

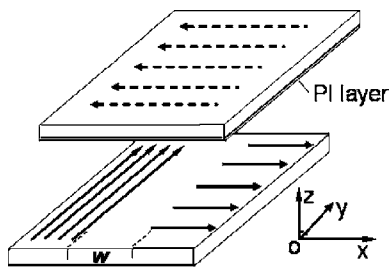


FIG. 1. Rubbing treatment on both substrate surfaces. The top surface is buffed along the  $x$  axis and the bottom surface is buffed in two indicated directions. The width of the nonrubbing zone on the bottom substrate is  $\sim 3.5$  mm. The cell gap is  $\sim 10$   $\mu\text{m}$ .

$$d\Delta n \gg \lambda/2. \quad (2)$$

If Eq. (2) is satisfied, then the transmitted light remains linearly polarized except that its polarization axis is rotated by  $90^\circ$  with respect to the incident one.

To demonstrate a LC polarization rotator, a cell according to the design of Fig. 1 was prepared. The top substrate surface was coated with a thin polyimide layer and buffed along the  $-x$  axis. The inner glass surface of the bottom substrate was rubbed gently. The width of the nonrubbed region is about  $w \sim 3.5$  mm. The cell gap was controlled using  $\sim 10$   $\mu\text{m}$  glass spacers. Merck nematic LC mixture BL003 ( $\Delta n = 0.261$  at  $\lambda = 589$  nm and  $T = 20^\circ\text{C}$ ) was injected to the empty cell in an isotropic state and afterwards the cell was cooled down gradually to room temperature ( $T \sim 21^\circ\text{C}$ ).

To confirm the above analysis, we examined the LC alignment by placing the cell between a polarizer and an analyzer. The rubbing direction of the top glass substrate was arranged parallel to the transmission axis of the linear polarizer and light is normally incident from the top substrate. When the optic axis of the analyzer was placed in parallel to that of the polarizer, the left side appeared black and the right side became bright, as shown in Fig. 3(a). This implies that the LC directors in the dark zone are twisted by  $90^\circ$  while the LC directors in the bright zone present a homogeneous alignment. Between these two distinct black and bright states, the transmitted light intensity changes gradually and continuous grayscales were observed. This region corresponds to the nonrubbed zone depicted in Fig. 2. By rotating the transmission axis of the analyzer in counterclockwise direction, the black strip gradually moves across the nonrubbed region. Figure 3(b) shows the black strip appearing at the

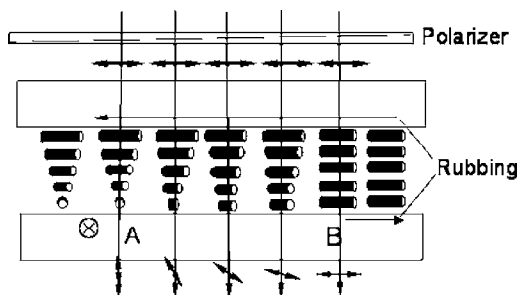


FIG. 2. LC director configurations in the cell. Positions A and B are the edges of the rubbing and nonrubbing regions. The left (right) surface of the bottom substrate to position A (B) is rubbed along the  $y$  ( $x$ ) axis. The surface between A and B on the bottom substrate has no rubbing treatment.

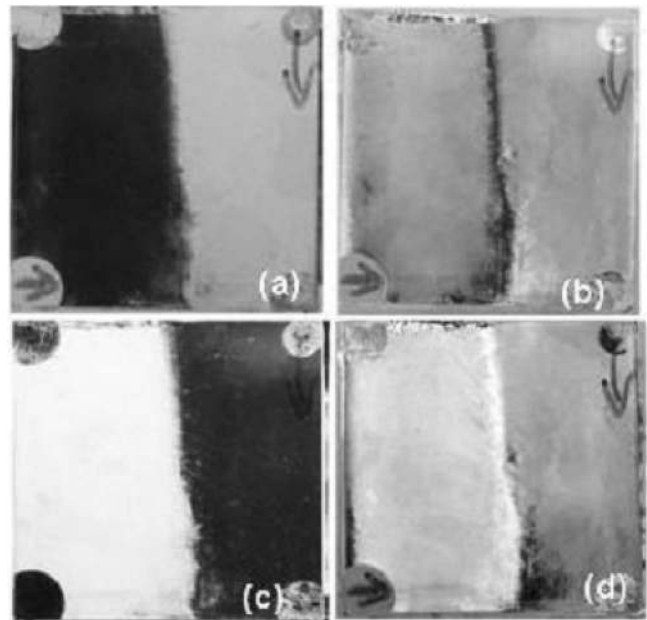


FIG. 3. Recorded intensity patterns of the LC rotator cell observed between a polarizer and an analyzer above a bright backlight. The rubbing direction of the top substrate is parallel to the axis of the polarizer. The axis of the polarizer is (a) parallel, (b)  $45^\circ$ , (c)  $90^\circ$ , and (d)  $135^\circ$  counterclockwise rotated.

center of the nonrubbed region when the analyzer was rotated by  $45^\circ$ .

When the analyzer was crossed to the polarizer, the left region became bright and the right region became black, as shown in Fig. 3(c). Continuously rotating the analyzer, a bright strip appears and moves from left to right. Figure 3(d) shows the case when the analyzer was rotated by  $135^\circ$ . Such results can be easily explained using Fig. 2.

To verify that the LC cell indeed functions as a variable linear polarization rotator, we first measured the light transmittance of the cell in the region where LC presents a continuous twist using a He-Ne laser ( $\lambda = 633$  nm). The cell was placed between crossed polarizers and the laser beam was incident normally on the cell from the uniformly rubbed side. The transmitted light was measured using a photodiode detector which was placed right behind the sample. To control the position of the cell, we mounted the cell on a linear translational stage. The dots in Fig. 4 represent the measured position-dependent transmittance of the LC cell in the central region. In the region from 0 to 0.75 mm, the He-Ne laser beam is located in the position where the LC directors ex-

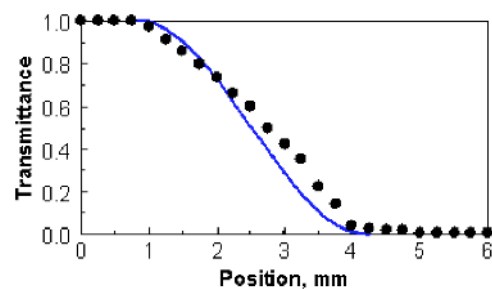


FIG. 4. (Color online) Normalized transmittance of the LC linear polarization rotator as a function of laser beam position. The dots and solid line are the measured data and simulated results, respectively.  $\lambda = 633$  nm and beam spot diameter is  $\sim 0.7$  mm.

hibit a  $90^\circ$  twist. Therefore, the transmittance is the highest. When the LC cell was translated along the  $x$  axis, the LC twist angle became smaller, as Fig. 2 shows, so that the transmittance was decreased gradually. As the position gets larger than  $\sim 4.25$  mm, the laser beam was almost completely blocked by the analyzer. This means that the laser beam is located in the region where LC presents a homogeneous alignment. From Fig. 4, the transmittance decreases with respect to the sample position and the contrast ratio reaches  $\sim 200:1$ . The limited contrast ratio is attributed to the finite spot size ( $\sim 0.7$  mm) of the employed laser beam.

To validate the above measured results, we theoretically calculated the light transmittance of the LC cell. Under Mauguin's condition, the transmittance of the LC cell can be expressed as

$$T = T_o \cos^2 \left( \frac{\pi}{2} \left( \frac{x - 0.75}{4.25 - 0.75} \right) \right). \quad (3)$$

In Eq. (3),  $T_o$  represents the maximum transmittance and  $x$  the position  $0.75 \leq x \leq 4.25$  mm. The calculated results are shown in Fig. 4 as the solid line. The two curves match reasonably well. The main error is caused by the finite spot size of the laser beam.

In the continuous twist region shown in Fig. 2, the twist gradient  $G_w$  is mainly determined by the width of the non-rubbed region ( $w$ ) and the twist angles ( $\phi_1$  to  $\phi_2$ ) of the two rubbed regions. The twist gradient can be approximated as

$$G_w = \frac{\phi_1 - \phi_2}{w}. \quad (4)$$

In Eq. (4),  $\phi_1$  and  $\phi_2$  are determined by the two rubbing directions of the bottom substrate. If the rubbing directions are fixed, as Fig. 2 shows, then widening the nonrubbing

zone will decrease the twist gradient. However, if the width is too large, the continuous twist can no longer sustain. For a fixed cell gap ( $d \sim 10 \mu\text{m}$ ), we found that the LC cell can present a continuous twist in the nonrubbing region if  $w < 5$  mm. For  $w > 5$  mm, LC alignment in the nonrubbing region is seriously affected by the rubbing direction of the top substrate.

Besides a single device, we can also fabricate a linear polarization rotator array by controlling the rubbing patterns of each pixel.

In conclusion, we demonstrated a LC-based polarization rotator using a simple rubbing method. The device can continuously rotate the polarization axis of an incident linearly polarized light within  $90^\circ$  of range. In addition to a single rotator device, a micropolarization rotator array can also be fabricated by controlling the rubbing patterns of each pixel. Such a LC polarization rotator has potential applications in density beam splitters, variable filters, optical data storage, grating, and other optical components.

The authors would like to thank Yi-Hsin Lin of National Chiao Tung University, Taiwan, for experimental assistance and Haiqing Xianyu for useful discussion.

<sup>1</sup>S. T. Wu, U. Efron, and L. D. Hess, *Appl. Opt.* **23**, 3911 (1984).

<sup>2</sup>R. Yamaguchi, T. Nose, and S. Sato, *Jpn. J. Appl. Phys., Part 1* **28**, 1730 (1989).

<sup>3</sup>M. Stalder and M. Schadt, *Opt. Lett.* **21**, 1948 (1996).

<sup>4</sup>J. A. Davis, D. E. McNamara, D. M. Cottrell, and T. Sonehara, *Appl. Opt.* **39**, 1549 (2000).

<sup>5</sup>Y. H. Wu, Y. H. Lin, H. Ren, X. Nie, J. H. Lee, and S. T. Wu, *Opt. Express* **13**, 4638 (2005).

<sup>6</sup>R. Yamaguchi and S. Sato, *Appl. Phys. Lett.* **86**, 031913 (2005).

<sup>7</sup>H. Ren, Y. H. Lin, and S. T. Wu, *Appl. Phys. Lett.* **89**, 051114 (2006).

<sup>8</sup>M. Schadt and W. Helfrich, *Appl. Phys. Lett.* **18**, 127 (1971).

<sup>9</sup>M. C. Mauguin, *Bull. Soc. Fr. Mineral.* **34**, 71 (1911).